

Iridate Li_8IrO_6 : An Antiferromagnetic Insulator

Callista M. Skaggs,¹ Peter E. Siegfried,^{2,3} Chang-Jong Kang,^{4,5} Craig M. Brown,⁶ Fu Chen,⁷ Lu Ma,⁸ Steven N. Ehrlich,⁸ Yan Xin,⁹ Mark Croft,¹⁰ Wenqian Xu,¹¹ Saul H. Lapidus,¹¹ Nirmal J. Ghimire,^{2,3} Xiaoyan Tan^{*1}

¹Department of Chemistry and Biochemistry, George Mason University, Fairfax, Virginia, 22030, United States

²Department of Physics and Astronomy, George Mason University, Fairfax, Virginia, 22030, United States

³Quantum Science and Engineering Center, George Mason University, Fairfax, Virginia, 22030, United States

⁴Department of Physics, Chungnam National University, Daejeon, 34134, Republic of Korea

⁵Institute of Quantum Systems, Chungnam National University, Daejeon, 34134, Republic of Korea

⁶National Institute of Standards and Technology, Gaithersburg, Maryland, 20899, United States

⁷Department of Chemistry and Biochemistry, University of Maryland, College Park, MD 20742, United States

⁸NSLS-II, Brookhaven National Laboratory, Upton, NY, 11973, United States

⁹National High Magnetic Field Laboratory, Tallahassee, Florida, 32310, United States

¹⁰Department of Physics and Astronomy, Rutgers, The State University of New Jersey, Piscataway, New Jersey, 08854, United States

¹¹X-ray Science Division, Advanced Photon Source, Argonne National Laboratory, Lemont, Illinois, 60439, United States

Corresponding Author* E-mail: xtan6@gmu.edu

Page

Figure S1. PXD patterns (Cu K α , $\lambda = 1.5418 \text{ \AA}$) of experimental Li_8IrO_6 (a), post TGA-DSC Li_8IrO_6 (b), calculated Li_8IrO_6 (c), and calculated Li_2IrO_3 . Ir impurity is labeled with #	S2
Table S1. Summary of Rietveld refinement parameters of the second phase Li_2O	S2
Figure S2. Temperature dependent DSC curves.	S2
Figure S3. Experimental in-situ SPXD patterns of Li_8IrO_6 while cooling process from 1273 K to 298 K. The impurity IrO_2 is marked with symbol *	S3
Figure S4. FC magnetic susceptibility of Li_8IrO_6 with an applied magnetic field of 1 T and inverse magnetic susceptibility fit with the $1/(\chi - \chi_0) = (T - \Theta_w)/C$ equation.	S3
Figure S5. DOS of the NM phase with DFT GGA + SOC + U (= 4 eV) method.....	S4
Table S2. Summary of Li_8TO_6 compounds	S4

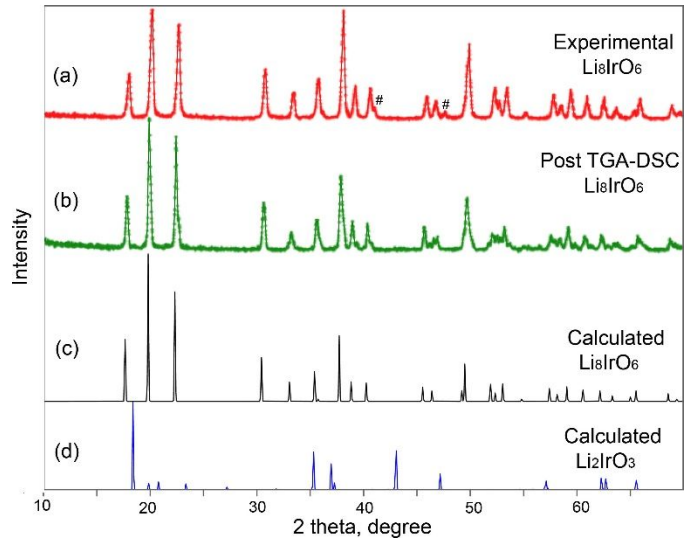


Figure S1. PXD patterns ($\text{Cu K}\alpha$, $\lambda = 1.5418 \text{ \AA}$) of experimental Li_8IrO_6 (a), post TGA-DSC Li_8IrO_6 (b), calculated Li_8IrO_6 (c), and calculated Li_2IrO_3 . Ir impurity is labeled with #.

Table S1. Summary of Rietveld refinement parameters of the second phase Li_2O . Values in parentheses indicate 1σ .

Phase	Unit cell parameters	x, y, z	Wyckoff symbol	$R_{\text{F-factor}}$	R_{brag} g	χ^2
Li_2O $Fm\bar{3}m$	$a = b = c = 4.6102(2) \text{ \AA}$ $\alpha = \beta = \gamma = 90^\circ$	Li: 0.25, 0.25, 0.25 O: 0, 0, 0	Li: 4a O: 8c	8.96	15.5	1.11

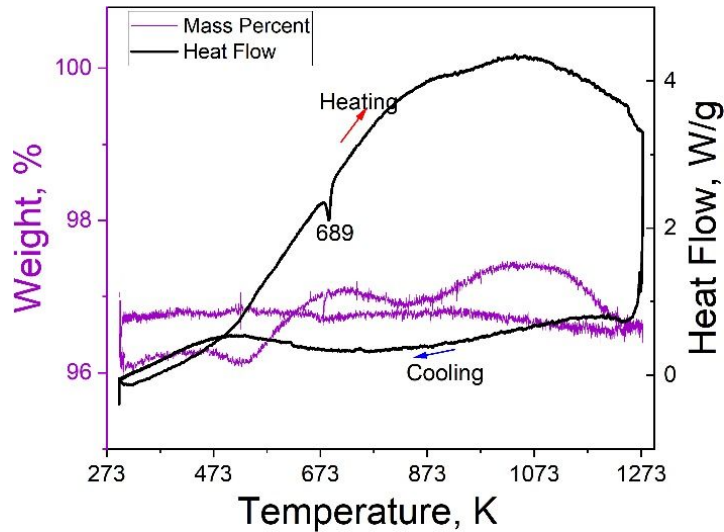


Figure S2. Temperature dependent TGA-DSC curves.

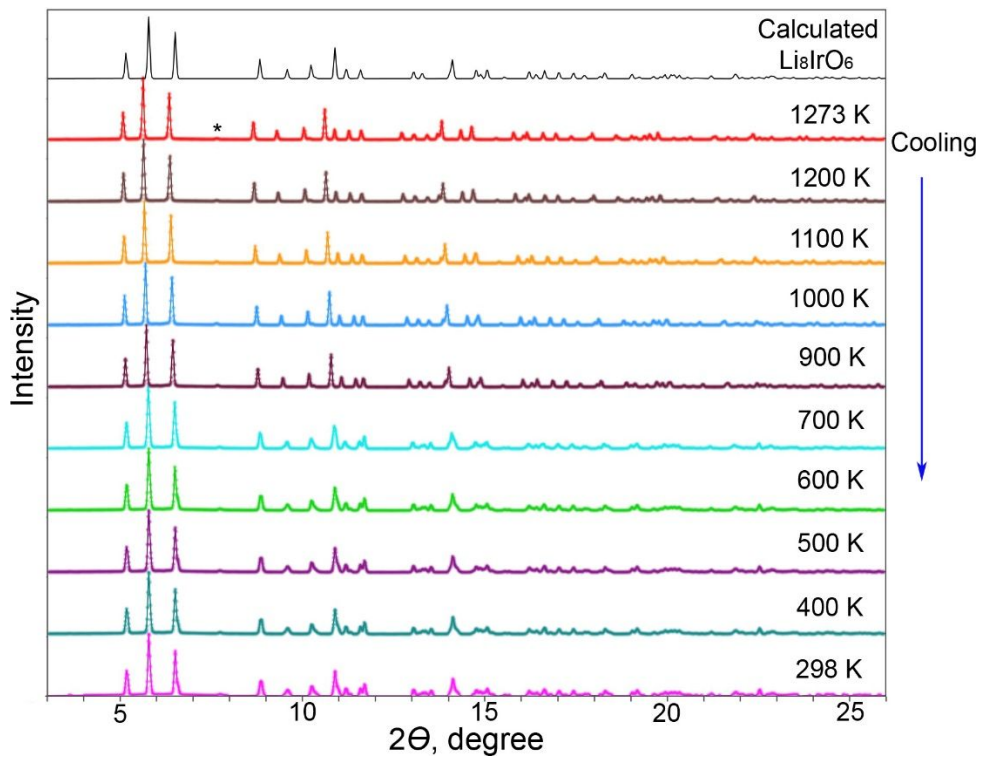


Figure S3. Experimental in-situ SPXD patterns of Li_8IrO_6 while cooling from 1273 K to 298 K. SiO_2 is marked with symbol *.

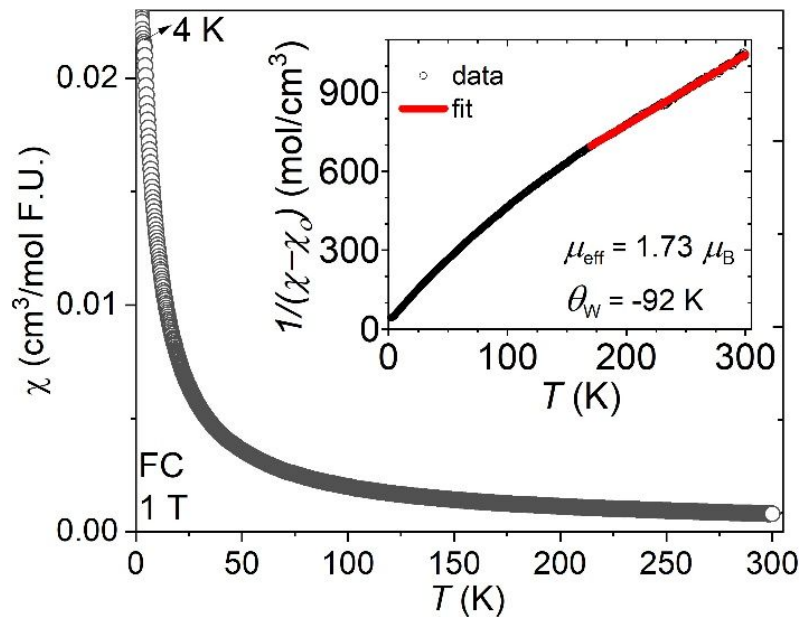


Figure S4. FC magnetic susceptibility of Li_8IrO_6 with an applied magnetic field of 1 T and inverse magnetic susceptibility fit with the $1/(\chi - \chi_0) = (T - \Theta_w)/C$ equation.

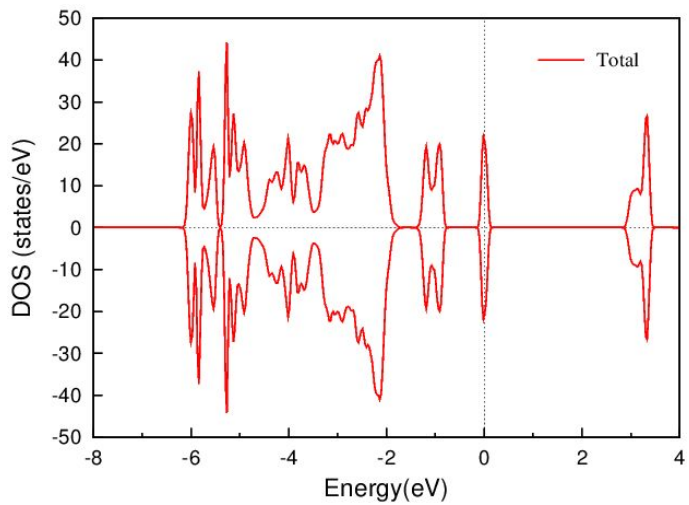


Figure S5. DOS of the NM phase with DFT GGA + SOC + U (= 4 eV) method.

Table S2. Summary of Li_8TO_6 compounds.¹⁴⁻²¹

Compound	$r(\text{T}^{4+})$, Å	Space Group
Li_8CeO_6	0.87	$R\bar{3}$
Li_8PrO_6	0.85	$R\bar{3}$
Li_8PbO_6	0.775	$R\bar{3}$
Li_8TbO_6	0.76	$R\bar{3}$
Li_8ZrO_6	0.72	$R\bar{3}$
Li_8HfO_6	0.71	$R\bar{3}$
Li_8SnO_6	0.69	$R\bar{3}$
Li_8PtO_6	0.625	$R\bar{3}$
Li_8IrO_6	0.625	$R\bar{3}$
Li_8RuO_6	0.62	$R\bar{3}$, tetragonal?
Li_8CoO_6	0.53	$P6_3mc$
Li_8GeO_6	0.53	$P6_3mc$
Li_8SiO_6	0.4	$P6_3mc$